Protonation Behavior of Histidine 24 and Histidine 119 in Forming the pH 4 Folding Intermediate of Apomyoglobin†

Bernhard Geierstanger,‡ Marc Jamin,‡ Brian F. Volkman,§ and Robert L. Baldwin*,‡

Department of Biochemistry, Stanford University School of Medicine, Stanford, California 94305-5307, and Department of Biochemistry and National Magnetic Resonance Facility, University of Wisconsin, Madison, Wisconsin 53706-1569

Received October 10, 1997; Revised Manuscript Received January 8, 1998

ABSTRACT: Heteronuclear NMR methods are used to study the protonation of histidine and aspartate residues in the acid-induced unfolding of recombinant sperm whale apomyoglobin. The results are combined with fluorescence and circular dichroism measurements of acid-induced unfolding of wild-type and double mutant (H24V/H119F) proteins. They are consistent with a simple model in which the failure to protonate a single buried histidine, H24, is largely responsible for the partial unfolding of native (N) wild-type apomyoglobin to the pH 4 folding intermediate (I). H24 is known to form an unusual interaction in which its side chain is buried and hydrogen-bonded to the side chain of H119. Two-dimensional $^{1}H-^{15}N$ heteronuclear NMR spectra indicate that H24 is present in the rare δ tautomeric form and remains neutral until N unfolds to I, while H119 becomes protonated before the N → I reaction occurs. In the H24V/H119F double mutant, all histidines are protonated in N and the N → I reaction occurs at lower pH. Therefore, the protonation of aspartate and/or glutamate residues must provide an additional driving force for the N to I reaction. Two-dimensional $^{1}H-^{13}C$ NMR experiments are used to measure the protonation of aspartates in selectively ^{13}C-labeled apomyoglobin; the results indicate that none of the aspartate residues has a strongly depressed pK_a in N, as would be expected if it forms a stabilizing salt bridge.

Native sperm whale apoMb[1] (N) unfolds at pH 4 to give an equilibrium folding intermediate, I (*1*). I contains a stable subdomain of N with intact A, G, and H helices (*2*). The pH 4 intermediate provides an attractive system for investigating the properties and roles of folding intermediates because I is also a rapidly formed (millisecond) transient intermediate in the refolding reaction of N at pH 6 (*3*). Moreover, I is formed cooperatively from the urea-unfolded protein at pH 4.2 (*4*−*6*). Also, I itself unfolds at acid pH in low salt and the N ⇌ I and I ⇌ U reactions can be conveniently separated from each other by pH change. Mutant studies of the urea-induced I ⇌ U transition at pH 4 indicate that I is stabilized by hydrophobic packing interactions qualitatively like those of N (*4*). The kinetics of the I ⇌ N reaction induced by pH change (pH 4 ⇌ pH 6) are measurable and show good reversibility (Jamin et al., manuscript in preparation). The partial unfolding of N to I involves the uptake of about two protons, and protonating the buried and hydrogen-bonded pair of histidine residues H24·H119 is thought to be chiefly responsible (*7*). The double mutant H24V/H119F is stable in the pH range near 4 where WT N unfolds to give I (*7*). Here we investigate the protonation behavior of His 24 and His 119 by NMR titration of the ^{15}N-labeled protein, using heteronuclear correlation NMR spectra that are optimized for the detection of histidine side chains (*8*).

The H24V/H119F double mutant forms I in a lower pH range where aspartate and glutamate residues become protonated. This means that Asp and/or Glu residues also contribute to driving the N → I reaction at acid pH. To understand the role of Asp residues both in the N → I reaction and the I → U reaction, we investigated the pH titration behavior of the aspartate residues using ^{13}C-labeled aspartate selectively incorporated into apoMb, together with heteronuclear NMR spectra correlating the chemical shifts of aspartate β-protons with those of the carboxylate carbons.

These NMR studies, combined with CD and fluorescence measurements of the unfolding of WT sperm whale apoMb and of the H24V/H119F double mutant, are used to model the pH dependence of the N ⇌ I reaction both in WT and in the H24V/H119F double mutant.

MATERIALS AND METHODS

Protein Expression and Purification. Uniformly ^{15}N-labeled wild-type sperm whale apoMb was prepared and

†This work was supported by the Deutsche Forschungsgemeinschaft (Ge 868/1-1 to B.H.G.) and the National Institutes of Health (GM-19988 to R.L.B. and GM-35976 to B.F.V.). The National NMR Facility at the University of Wisconsin at Madison (RR02301) is acknowledged for the use of their instruments and for staff support.

* To whom correspondence should be addressed.

‡ Stanford.

§ University of Wisconsin.

[1] Abbreviations: CD, circular dichroism; NMR, nuclear magnetic resonance; Mb, myoglobin; apoMb and holoMb, apo- and holomyoglobin; N, I, and U, native, intermediate, and acid-unfolded forms of apomyoglobin; WT, wild-type; CO, carbon monoxide; HMBC; heteronuclear multiple bond correlation; 1D and 2D, one- and two-dimensional.

S0006-2960(97)02516-6 CCC: $15.00
Published on Web 03/07/1998

purified as described previously (*9*). Unlabeled protein (*7*) was prepared by constitutive expression in *Escherichia coli* TB1 cells in rich LB medium. To obtain ^{15}N-labeled H24V/H119F double mutant protein, the mutated gene (*7*) was transferred into a T7 expression plasmid. Labeled apoMb was overexpressed using *E. coli* strain BL21(DE3) (Novagen) grown in minimal M9 medium (*10*) supplemented with ^{15}N ammonium chloride (Isotec) at 37 °C in Fernbach flasks. Expression and purification followed the protocol described earlier (*9*).

Aspartates in wild-type and H24V/H119F apoMb were specifically ^{15}N,^{13}C-labeled using the T7 expression plasmid in *E. coli* EA-1 cells that are deficient in aspartate synthesis and transaminase activity (*aspC*$^-$ *asnA*$^-$ *asnB*$^-$ *tyrB*$^-$). This strain was kindly provided by Professor John Markley (University of Wisconsin, Madison). To incorporate ^{13}C-labeled aspartic acid, M9 medium was supplemented with 125 mg/L uniformly [^{15}N,^{13}C]-labeled D,L-aspartic acid (96% ^{13}C, 99% ^{15}N) (Cambridge Isotopes) and the following concentrations of L-amino acids (Sigma): approximately 60 mg/L, His, Ile, Leu, Lys, Pro, Thr, Val, Tyr, Phe, Trp, Cys, and Cys_2; 160 mg/L, Glu and Met; 250 mg/L: Ala, Arg, Gly, Gln, and Asn; and 1000 mg/L, Ser. Amino acids were either added in form of a 0.5 mg/mL stock solution or in powder form. In addition, the medium contained approximately 1.25 g/L NH_4SO_4, 12.5 g/L glucose, 125 mg/L carbenicillin, 25 mg/L thiamin, 0.5 mL of vitamin mix/per L of medium, 2.5 mM $MgSO_4$, and 0.125 mM $CaCl_2$ and $FeCl_3$ as well as 60 mg/L δ-aminolevulinic acid hydrochloride (Sigma) as heme precursor. Protein expression was induced with 60−100 mg/L dioxane-free isopropyl β-D-thiogalactopyranoside (IPTG) (Sigma) at an OD_{600} of approximately 0.8 after cells were grown at 37 °C in Fernbach flasks. At this point an additional 100 mg/L DL-[U-^{15}N,^{13}C]-aspartic acid as well as another equivalent of all other amino acids were added. After an additional 6−8 h of vigorous shaking at 30 °C, the cells were harvested by centrifugation. All protein preparations were >95% pure after purification (*9*) according to SDS−polyacrylamide gel electrophoresis.

NMR Sample Preparation. Lyophilized protein was dissolved in 10 mM acetic acid-d_3 or 2 mM citric acid in D_2O by inverting an eppendorf tube in the cold room at 8 °C. The pH* of the sample (initially pH* 3.8−4.0) was adjusted by adding small amounts of 0.4% NaOD or 0.35% DCl. Samples were stored at 4 °C. Protein concentrations varied between 8 and 17 mg/mL (sample volume 0.5 mL), corresponding to approximately 0.5−1 mM.

NMR Experiments. One-dimensional ^{1}H spectra were acquired in D_2O at 25 and 35 °C using 4096 complex points over a spectral width of 6006 Hz. Two hundred fifty-six scans were typically recorded with a 2 s presaturation pulse for solvent suppression. ^{1}H−^{15}N HMQC NMR experiments (*11*) (referred to as HMBC experiments hereafter) with uniformly ^{15}N-labeled protein were optimized for the detection of histidine residues as described (*8*) using a 22 ms delay between the first 90° pulses at the proton and nitrogen frequency. The residual HDO line was suppressed with a low-power presaturation pulse during the recycling delay of 1 s. Either 256 or 512 complex t_1 experiments with 48−512 scans were recorded with spectral widths of 5000 Hz in the nitrogen dimension and 6006 Hz in the proton dimension. Nitrogen−proton coupling was suppressed during data acquisition using a Waltz16 decoupling pulse train (*12*). Assignment of the cross-peaks was achieved by using the histidine proton assignments of Lecomte and co-workers (*13, 14*) reported at 25 °C for sperm whale apoMb for all histidines except H64. H64 assignments were from horse apoMb (*13*). Assignments could be transferred to 35 °C because of the similarity in pK_a values and relative peak arrangement. Modified ^{1}H−^{13}C CT-HCACO experiments (*15, 16*), abbreviated as 2D ^{1}H−^{13}C HBCBCO hereafter, were used to determine the titration behavior of ^{13}C-labeled aspartic acid residues in apoMb. Sixty-four complex t_1 experiments with 128 scans were recorded with spectral widths of 2500 Hz in the carbon dimension and 6250 Hz in the proton dimension. Spectra were referenced to the HDO line at 4.76 ppm (25 °C) and 4.66 ppm (35 °C). All pH values are the uncorrected readings of a Mettler Toledo NMR pH electrode at room temperature.

Fitting of NMR Titration Data. pK_a values of histidine and aspartates were determined by fitting ^{1}H, ^{15}N, and ^{13}C chemical shift values (δ) as a function of pH to the Henderson−Hasselbalch equation:

$$\delta(\mathrm{pH}) = \delta(\text{neutral form}) + \Delta\delta[10^{n(\mathrm{p}K_a-\mathrm{pH})}]/[1 + 10^{n(\mathrm{p}K_a-\mathrm{pH})}]$$

using KaleidaGraph 3.0 ($\Delta\delta$ is the chemical shift difference between charged and neutral forms). To fit the limited number of data points, the chemical shift of the neutral β-type nitrogen was set to 240 or 250 ppm. The number of protons n was typically set to 1.

pH Titrations Monitored by Circular Dichroism and Fluorescence Spectroscopy. CD data of protein samples of 2 μM in 2 mM sodium citrate were acquired at 222 nm using a 1 cm path length cuvette on an Aviv 60DS circular dichroism spectropolarimeter at 35 °C. Fluorescence measurements were performed at 35 °C with a SLM-Aminco Bowman Series 2 luminescence spectrometer. Excitation occurred at 288 nm while fluorescence emission spectra were recorded from 320 nm to 380 nm with 1 nm/sec using a 1 cm × 0.5 cm cuvette. Protein concentrations were 2 ± 0.2 μM in 2 mM sodium citrate. Small amounts of hydrochloric acid were added to obtain samples at low pH values. The fluorescence signal was corrected for the small differences in protein concentration. For wild-type and H24V/H119F double mutant protein, fluorescence data points above pH 5.8 were not included in the fitting. For reasons that are currently under investigation, the CD and the fluorescence values for the native state of mutant and wild-type protein vary significantly.

Modeling of the Acid-Induced Unfolding of Apomyoglobin As Monitored by Circular Dichroism and Fluorescence Spectroscopy. The acid-induced unfolding of apoMb was modeled with a simple sequential three-state model (N ⇌ I ⇌ U). The model described previously (*7, 17*) was modified to include the NMR-derived pK_a values of individual titrating groups. All 12 histidines, 14 glutamates, and seven aspartates in apoMb were considered to be independent proton binding sites. By use of KaleidaGraph 3.0, the CD and fluorescence data shown in Figure 2 were fitted to

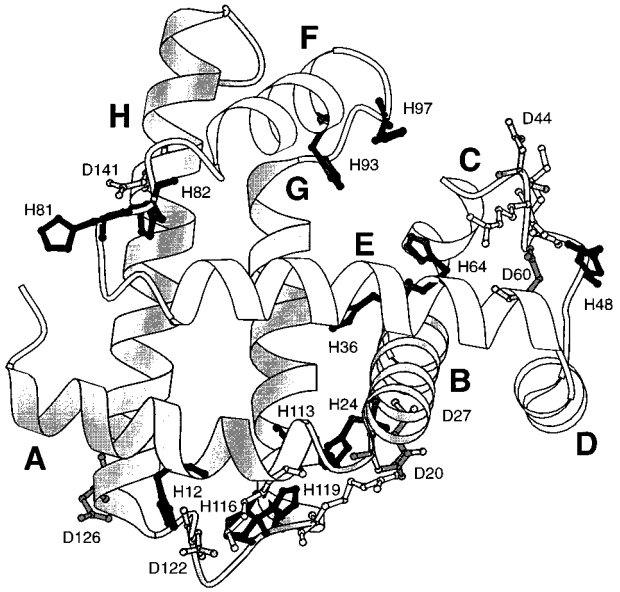

FIGURE 1: MOLSCRIPT diagram (*48*) of sperm whale myoglobin (from the X-ray structure of holomyoglobin; *44*). The A, B, G, and H helices are highlighted in gray. Histidine side chains are shown as dark ball-and-stick models, while lightly shaded side chains show aspartate residues and their salt bridge partners.

$$\mathrm{FL(pH)} = (\mathrm{FL_N} + \mathrm{FL_I}K_{\mathrm{NI}} + \mathrm{FL_U}K_{\mathrm{NI}}K_{\mathrm{IU}})/(1 + K_{\mathrm{NI}} + K_{\mathrm{NI}}K_{\mathrm{IU}}) \quad (1)$$

$$\mathrm{CD(pH)} = (\mathrm{CD_N} + \mathrm{CD_I}K_{\mathrm{NI}} + \mathrm{CD_U}K_{\mathrm{NI}}K_{\mathrm{IU}})/(1 + K_{\mathrm{NI}} + K_{\mathrm{NI}}K_{\mathrm{IU}}) \quad (2)$$

with

$$K_{\mathrm{NI}} = K_{\mathrm{NIref}}P_{\mathrm{I}}/P_{\mathrm{N}} \quad (3)$$

$$P_{\mathrm{I}} = [1 + 10^{(\mathrm{p}K_{\mathrm{a}}\mathrm{His_I} - \mathrm{pH})}]^{n_{\mathrm{His}}} \times \{1 + 10^{[\mathrm{p}K_{\mathrm{a}}(\mathrm{Glu+Asp})_{\mathrm{I}} - \mathrm{pH}]}\}^{n_{(\mathrm{Glu+Asp})}} \quad (4)$$

$$P_{\mathrm{N}} = \{\Pi[1 + 10^{(\mathrm{p}K_{\mathrm{a}}\mathrm{His_N}^{i} - \mathrm{pH})}]^{n_{\mathrm{His}}{}^{i}}\} \times \{1 + 10^{[\mathrm{p}K_{\mathrm{a}}(\mathrm{Glu+Asp})_{\mathrm{N}} - \mathrm{pH}]}\}^{n_{(\mathrm{Glu+Asp})}} \quad (5)$$

$$K_{\mathrm{IU}} = K_{\mathrm{IUref}}\{1 + 10^{[\mathrm{p}K_{\mathrm{a}}(\mathrm{Glu+Asp})_{\mathrm{U}} - \mathrm{pH}]}\}^{n_{(\mathrm{Glu+Asp})}}/\{1 + 10^{[\mathrm{p}K_{\mathrm{a}}(\mathrm{Glu+Asp})_{\mathrm{I}} - \mathrm{pH}]}\}^{n_{(\mathrm{Glu+Asp})}} \quad (6)$$

$K_{\mathrm{NI}}{}^{\mathrm{ref}}$ and $K_{\mathrm{IU}}{}^{\mathrm{ref}}$ are the reference equilibrium constants for the N ⇌ U and I ⇌ U equilibria at high pH values, respectively. $\mathrm{FL_N}$, $\mathrm{FL_I}$, $\mathrm{FL_U}$ and $\mathrm{CD_N}$, $\mathrm{CD_I}$, $\mathrm{CD_U}$ represent the fluorescence (FL) and circular dichroism signals in N, I, and U states. $n_{(\mathrm{E+D})}$ is the number of aspartates and glutamates, n_{H} is the number of histidines. $\mathrm{p}K_{\mathrm{a}}(\mathrm{E} + \mathrm{D})_{\mathrm{N}}$, $\mathrm{p}K_{\mathrm{a}}(\mathrm{E} + \mathrm{D})_{\mathrm{I}}$, and $\mathrm{p}K_{\mathrm{a}}(\mathrm{E} + \mathrm{D})_{\mathrm{U}}$ are the $\mathrm{p}K_{\mathrm{a}}$ values of aspartates and glutamates in N, I, and U states. All aspartates and glutamates were considered to have the same $\mathrm{p}K_{\mathrm{a}}$ values. $\mathrm{p}K_{\mathrm{a}}\mathrm{H_I}$ is the $\mathrm{p}K_{\mathrm{a}}$ values of all histidines in I, while $\mathrm{p}K_{\mathrm{a}}\mathrm{H_N}^{i}$ represents the $\mathrm{p}K_{\mathrm{a}}$ value of individual or groups of histidines in N. NMR data show (see below) that all histidines are protonated in I. Protonation of histidines, therefore, does not play a role in the I → U transition. Consequently, K_{IU} contains only terms for the titration of aspartates and glutamates.

RESULTS

Acid-Induced Unfolding of Wild-Type and H24V/H119F Double Mutant Apomyoglobin Monitored by Circular Dichroism and Fluorescence Spectroscopy. The replacement of H24 and H119 in sperm whale apoMb by nonpolar residues (*7*) has profound effects on the pH dependence of the acid-induced unfolding reaction. Figure 2 shows pH titrations of wild-type and H24V/H119F apoMb monitored by circular dichroism (CD) and fluorescence spectroscopy at 35 °C. For wild-type apoMb, the transition N ⇌ I occurs with a pH midpoint of approximately 4.4. The transition is marked by a decrease in CD but by an increase in fluorescence signal. I unfolds to the acid-unfolded form U with a pH midpoint of 3.2. The acid-induced formation of I is not well resolved by CD but I is resolved by including urea (*7*) as well as by monitoring unfolding by fluorescence (Figure 2B). Figure 2B also shows that the midpoint of the N ⇌ I transition of H24V/H119F is shifted to lower pH with a maximum fluorescence at pH 3.2. From the fluorescence data, as well as from fitting the CD data to the three-state model (N, I, and U) (*17*), it appears that the intermediate is only partially populated for H24V/H119F apoMb.

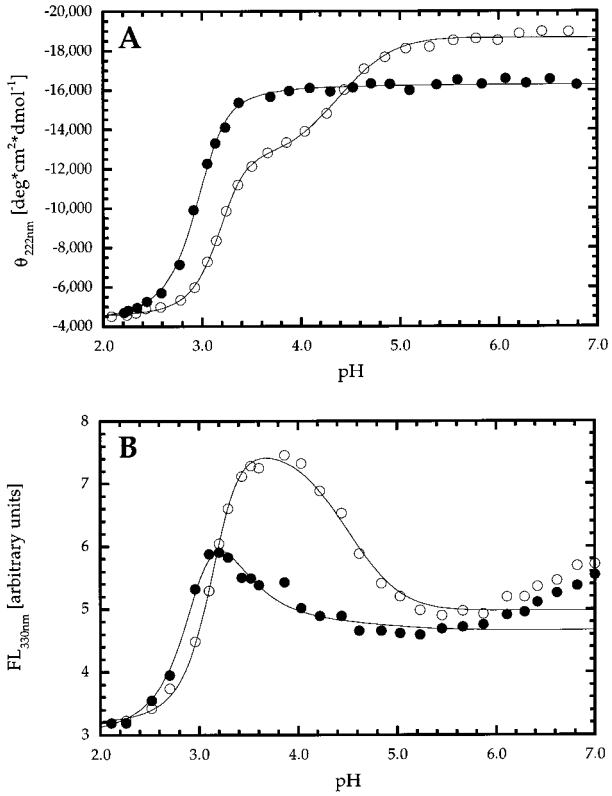

FIGURE 2: Effects of histidine mutations on the acid-induced unfolding transition of apomyoglobin (in 2 mM sodium citrate at 35 °C). pH titration as monitored by circular dichroism (A) and fluorescence spectroscopy (B) for wild-type (○) and H24V/H119F double mutant protein (●). Lines represents the fits of the data using the titration model described in the text. $\mathrm{p}K_{\mathrm{a}}$ values for the 12 histidines were fixed according to the NMR data to the following values: H119 and H113, 6.0; H12, H81, H116, H93, H97, and H82, 6.5; H36, 8.0; H64, 5.0; H48, 5.5; and H24, 3.0. The seven aspartates and 14 glutamates are assumed to have the same $\mathrm{p}K_{\mathrm{a}}$ value: 3.3 in N, 3.4 in I, and 3.7 in U. Fluorescence data were obtained with identical instrument settings and were normalized to compensate for small differences in protein concentration (<10%). For reasons that are currently under investigation, the CD value for native H24V/H119F (above pH 6) is lower than that of wild-type. Similarly, the increase of the fluorescence signal in N at pH values above 5.8 is not understood at present.

Protonation Behavior and Tautomeric State of Histidines in Wild-Type Apomyoglobin Monitored by $^{1}H-^{15}N$ NMR

Chart 1

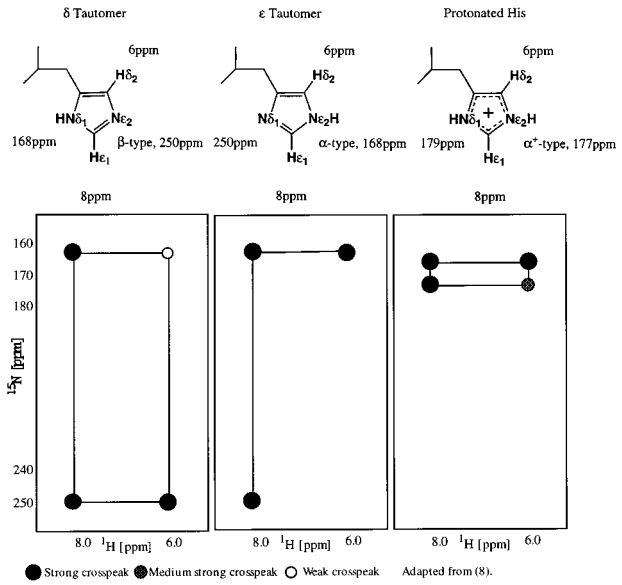

Spectroscopy. Heteronuclear $^1H-^{15}N$ correlation NMR spectroscopy is used here to determine the pK_a values of histidines in apoMb. Both the nitrogen chemical shift values of histidine side chains and the cross-peak patterns are highly characteristic for the protonation and the tautomeric states of histidine side chains: see Chart 1 (*8, 18*). Two-dimensional $^1H-^{15}N$ HMBC spectra, optimized as described (*8*) to detect histidine side chains in uniformly ^{15}N-labeled apoMb, were acquired between pH 2.5 and 9.4 at 25 and 35 °C. The $^1H-^{15}N$ cross-peaks are assigned on the basis of the proton assignments of Lecomte and co-workers for histidines in wild-type sperm whale and horse apoMb (*13, 14*) reported at 25 °C. Assignments could be transferred to 35 °C because of the similarity in pK_a values and relative peak arrangement. The tautomers of the histidine residues in holoMb were assigned by Lecomte and co-workers in a paper (*19*) published after this paper was submitted (see also ref *20*).

The $^1H-^{15}N$ HMBC cross-peaks of histidine side chains are well resolved in N (Figure 3A). In the N ⇌ I transition zone, resonances of both N and I are present, indicating that N and I interchange slowly on the NMR time scale (Figure 3B). Below pH 4.6, the cross-peak intensities for N are too weak to be detected. All observable histidines are protonated in I at pH 4.2, and some chemical shift dispersion remains in both ^1H and ^{15}N dimensions (Figure 3D). As the pH is lowered, the cross-peaks gradually shift to their positions in the completely acid-denatured form, in which all chemical shift dispersion is lost (Figure 3E). At pH values above 6.8, the lines in the ^{15}N dimension of most histidines are exchange-broadened beyond detection (see below and Figure 3C). Comparison of the ^{15}N chemical shifts in holoMb and native apoMb (data not shown) indicates that the ^{15}N chemical shift is chiefly dictated by the protonation state of the histidines.

$^1H-^{15}N$ HMBC cross-peak patterns unambiguously identify the tautomer of a histidine side chain (Chart 1). In particular, these patterns allow us to investigate the titration of the special histidine pair H24·H119 that apparently plays a key role in the acid-induced partial unfolding of apoMb (*7*). Because of the hydrogen bonding between their side chains, H24 and H119 are expected to have strongly coupled titrations (*13, 14, 21*). In the $^1H-^{15}N$ HMBC NMR spectra (Figure 3A), all histidines except H24 show cross-peak patterns that are expected for the ϵ tautomeric state (Chart 1) (*8*), which is the energetically preferred tautomer in free histidine (*18*). H24 shows two strong cross-peaks between the aromatic protons and a β-type nitrogen (nitrogen with a lone electron pair) at around 242 ppm and two weaker peaks with an α-type nitrogen (nitrogen with proton bound in neutral histidine) at 171 ppm. This pattern confirms that H24 is neutral and in the δ tautomer at all pH values between 4.6 and 9.6. The structure of native apoMb at pH 6 is similar to that of holoMb except in the region of the empty heme binding pocket (*1, 2, 13, 22−24*). As in holoMb, histidine H24 (B helix) is, therefore, presumably fixed in its position by strong hydrogen-bonding interactions with the side chain of H119 (helix G) and with the backbone CO of aspartate D20 (*14, 24−26*) and by the presence of the guanidinium group of R118 that sits right above the ring of H24 (Figure 1) in holoMb. In contrast to H24, its hydrogen-bonding partner H119 is partially titrated and exists in the ϵ tautomer at pH 5.7 (Figure 3A) but is almost completely protonated at pH 4.6 (Figure 3B). The changes in ^{15}N and ^1H chemical shift of the histidine side chains of wild-type apoMb as a function of pH are displayed in Figure 4, and pK_a values derived from fitting chemical shift values to the Henderson−Hasselbalch equation are listed in Table 1. The pH titration shows that H119 titrates with a pK_a of 6.0 ± 0.1, close to the value of 5.8 reported from ^1H NMR data (*14*) and similar to the value in the CO form of holoMb (*21*). The β-type nitrogen chemical shift clearly indicates that H24 remains neutral over the whole pH range. Small chemical shift changes observed for the H24 resonances reflect the titration of the neighboring H119 residue. The pK_a of H24 must be significantly below 4.0 in N but cannot be estimated more accurately since N is not populated at pH 4 or below.

In agreement with previous results (*13, 14*), the remaining histidines of apoMb can be classified into the following groups (Tables 1 and 2): (a) H81, H116, and H12 titrate with pK_a values of about 6.5, about that of unperturbed histidine residues. (b) H113 and H48 titrate with somewhat lower pK_a values, around 6.0 and 5.5, respectively. (c) H36 has an unusually high pK_a, presumably caused by a charge−aromatic interaction with the nearby phenylalanine ring of F106 and by an electrostatic interaction with the acidic side chain of E38 (*7, 14, 21*). Our limited data do not extend sufficiently far into the transition zone to estimate the pK_a value, but Lecomte and co-workers (*14*) report a value of 8.2 from their more extensive 1D ^1H NMR data. (d) H93, H97, and H82, which line one side of the empty heme binding pocket, could not be observed, as discussed below. (e) For the distal heme ligand H64, a pK_a value around 4.8 is estimated; this low value presumably is caused by the nearby positively charged side chain of arginine R45.

All titration curves were fitted assuming binding of a single proton, i.e., $n = 1$. The titration of the H64 δ1 nitrogen shows the influence of neighboring groups, however. If the end points are 240−250 ppm for the neutral form and 178−190 ppm for the charged form, then the δ1 nitrogen chemical shift of 201.9 ppm (Figure 4A) suggests that H64 is protonated between 60% and 80% at pH 4.65 and has a pK_a

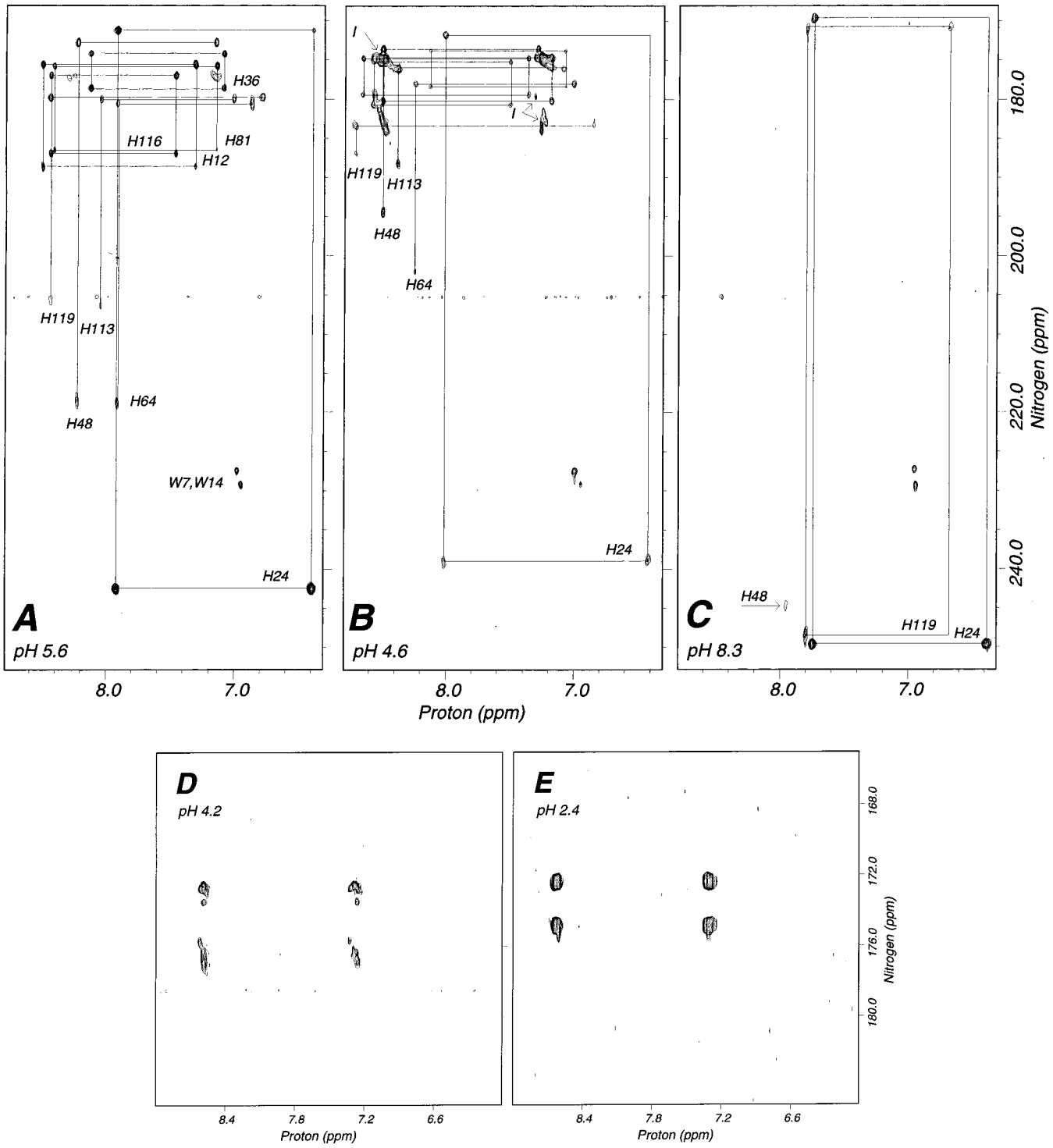

FIGURE 3: $^{1}H-^{15}N$ HMBC NMR spectra of ^{15}N-labeled wild-type apomyoglobin acquired at 35 °C (10 mM sodium acetate in D_2O) at 500 MHz. (A) Spectra of native apomyoglobin at pH 5.6. (B) Spectra at pH 4.6 indicating a mixture of N and I. The cross-peaks for H24, H119, and H64 in the native form are highlighted. Arrows point to the upper left and lower right cluster of peaks of the protein in the intermediate form. (C) Spectra at pH 8.3. Only cross-peaks for H119, H24, and H48 are observed above pH 6.8 because of exchange broadening of the ^{15}N resonances of all other histidines (see text). The cross-peaks W7 and W14 are caused by the indole nitrogen of tryptophan 7 and 14. (D) Expanded region of spectra of apomyoglobin in the intermediate form at pH 4.2 and 25 °C. (E) Expanded region of spectra of unfolded apomyoglobin at pH 2.4 and 25 °C. All peaks in the spectra of intermediate and unfolded apomyoglobin show the characteristic chemical shifts and cross-peak patterns of fully protonated histidine side chains (see text).

value between 4.7 and 4.9. The chemical shift behavior of the H64 ϵ2 nitrogen is consistent with this pK_a value (Figure 4B). The data fitting can be improved by assuming that the titration of H93 and H97 affect the δ1 nitrogen chemical shift of H64 by 5−20 ppm. In holoMb, the ϵ2 nitrogen of H97 is approximately 8.2 Å from ϵ2 of H64, while for H93 the corresponding distance is approximately 6.6 Å. In apoMb these side chains are presumably closer, at least part of the time, because of conformational exchange, as discussed below. The fit of the titration data for H64 improves if either one or two neighboring histidines with pK_a values of 6.0−7.0 are allowed to affect the curve. This procedure

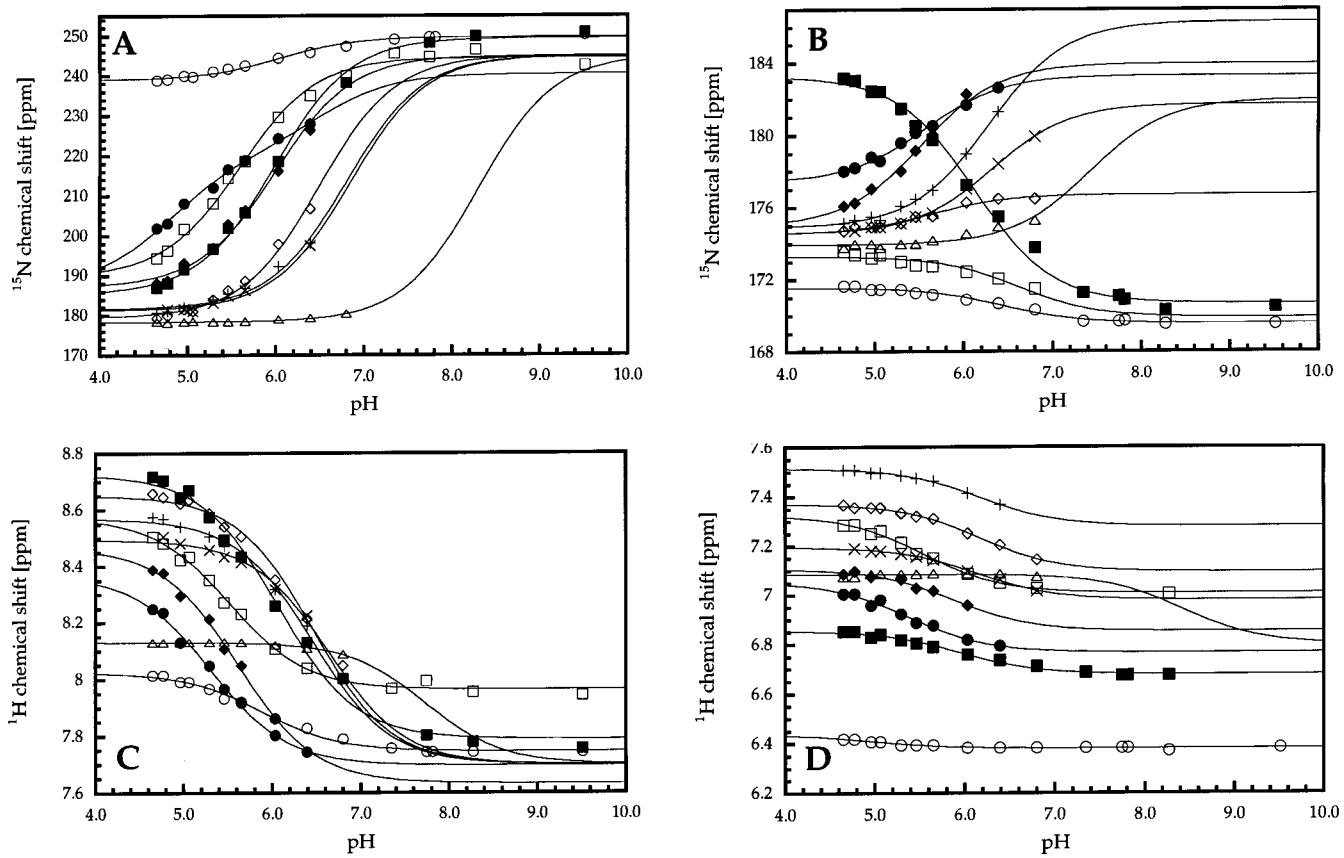

FIGURE 4: ^{15}N and ^{1}H chemical shift values of the detectable histidine side chains in native wild-type apomyoglobin at various pH values (from ^{1}H−^{15}N HMBC spectra at 35 °C, 10 mM sodium acetate in D_2O). (A) δ1 nitrogen (except for H24 ϵ2 nitrogen), (B) ϵ2 nitrogen (except for H24 δ1 nitrogen), (C) ϵ1 proton, and (D) δ2 proton. H24 (○), H119 (■), H48 (□), H36 (△), H64 (●), H113 (◆), H81 (×), H116 (+), H12 (◇). Lines represent the fits of the Henderson−Hasselbalch equation using the parameters described in Table 1.

Table 1: Histidine pK_a Values in Wild-Type Sperm Whale Apomyoglobin

residue fit based on[a]	pK_a $^{15}N^{\delta1}$	range[b]	$^{15}N^{\epsilon2}$	$^{1}H^{\epsilon1}$	$^{1}H^{\delta2}$	pK_a apoMb[c]	pK_a holoMb[d]
H12	6.5[e]	6.1−6.5 (6.1)	5.6	6.3−6.6[f]	6.2	6.4	6.29, 6.26
H24[g]	(6.0)		(6.4)	(5.9)	(4.9)	<4.8	6.2, <4.5
H36[h]	(8.3)[e]		(7.4)	(7.6)	(7.9)	8.2	8.06, 7.91
H48	5.6		6.6	5.5	5.5	5.2	5.25, 5.30
H64[i]	4.8	(5.3)	(5.6)	(5.3)	(5.4)	<5.0	<5.0
H81	6.8[e]	6.50−6.89 (6.2)	6.3	6.5−6.7[g]	6.1	6.5	6.68, 6.53
H82	n.o.[j]		n.o.	n.o.	n.o.	n.o.	<5, <5
H93	n.o.		n.o.	n.o.	n.o.	n.o.	<5, <5
H97	n.o.		n.o.	n.o.	n.o.	n.o.	5.63
H113	6.0[e]	5.6−6.1 (5.8)	5.5	5.6	5.9	<5.5	5.44, 5.36
H116	6.8[e]	6.5−6.8 (6.1)	6.3	6.4−6.5[g]	6.2	6.6	6.49, 6.50
H119	6.0		6.1	6.1	6.0	5.3−5.8	6.13, 6.13

[a] Present study, derived from ^{1}H−^{15}N HMBC data at 35 °C (see text). Fixed: n=1. Chemical shift end points for charged and neutral species were free to floatunless noted otherwise. [b] Fixed end point at high pH: δ = 220−250 ppm for H12, H36, H81, and H116; δ = 230−250 ppm for H113, R better than 0.97, value in parentheses is for n = 1 and end points free. [c] References *13* and *14*, ^{1}H NMR data at 298 K. [d] Values for the carbonmonoxy form of myoglobin were determined at 35 °C by Bashford et al. (*21*). [e] Fixed end point at high pH: δ = 245 ppm. [f] Range for various fixed end points. [g] pK_a reflects titration of neighboring H119. [h] There are too few data points to estimate the pK_a value of H36. Values in parentheses are for fixed end points at high pH. [i] Titration of H64 results from the coupled titration of more than one histidine; see text.Titration of $^{15}N^{d}1$ can be fitted by considering a fixed pK_a = 4.8 (n = 1) for H64 and the titration of a second histidine with pK_a = 6.5 (n = 1, end points and $\Delta\delta$ for second histidine free). The other values in parentheses are for free end points and n = 1. [j] n.o., not observed.

gives a pK_a between 4.5 and 5.2, consistent with the simple chemical shift argument.

The ϵ2 nitrogen of H119 also shows an unusual titration behavior (Figure 4B). The chemical shift difference between the protonated and neutral forms is 12 ppm, the largest difference observed in apoMb. The chemical shift of the H119 ϵ2 nitrogen increases to lower field as the pH is decreased, together with the H48 ϵ2 and H24 δ1 nitrogens. Simultaneously, the H24 ϵ2 nitrogen shifts upfield (Figure 4A), while the hydrogen-bond-donating δ1 nitrogen of H24 shifts downfield (Figure 4B). The magnitude and direction of the H24 shift suggest that the hydrogen bond between the H24 and H119 side chains increases in strength as H119 becomes protonated: Strong hydrogen bonds shift the resonance of a hydrogen-bond-accepting nitrogen up to 10 ppm upfield (smaller ppm value) but shift the resonances of

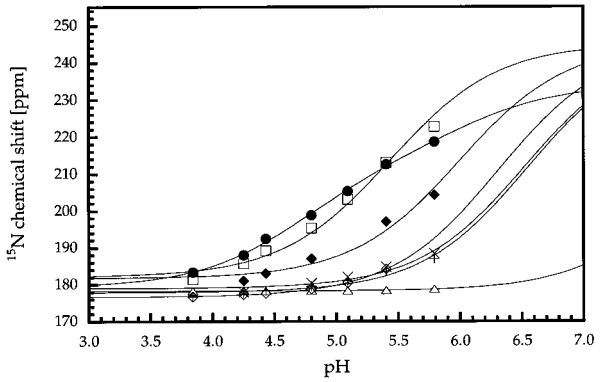

FIGURE 5: Titration data for H24V/H119F. ^{15}N chemical shift values of the δ1 nitrogen of all detectable histidine side chains in N at various pH values (from ^{1}H−^{15}N HMBC spectra at 35 °C, 2 mM sodium citrate in D_2O). H48 (□), H36 (△), H64 (●), H113 (◆), H81 (×), H116 (+), H12 (◇). Lines represent the fits of the Henderson−Hasselbalch equation resulting in the following pK_a values: H48, 5.4; H36, 7.9; H64, 4.9; H113, 6.0; H81, 6.5; H116, 6.5; and H12, 6.3. Depending on the settings, these values vary within the range observed for wild-type apomyoglobin (see Table 1).

Table 2: pK_a Values Used in Fitting CD and Fluorescence Data (Figure 2) for Wild-Type and H24V/H119F Mutant Apomyoglobin

residue	pK_a N	pK_a I	pK_a U
H12, H81, H82, H93, H97, H116	6.5	6.5	6.5
H24	3.0	6.5	6.5
H36	8.0	6.5	6.5
H48	5.5	6.5	6.5
H64	5.0	6.5	6.5
H113	6.0	6.5	6.5
H119	6.0	6.5	6.5
D (all seven aspartates)	3.3	3.4	3.7
E (all 14 glutamates)	3.3	3.4	3.7

the H-bond donor nitrogen downfield (larger ppm value) (*27*−*33*). At high pH the ϵ2 nitrogens of H48 and H119 and the δ1 nitrogen of H24 are at least 6 ppm upfield of the protonated nitrogens of all other histidines. For H119 and H24 this behavior may be caused by the buried nature of these side chains, because the chemical shift of α-type nitrogens shifts up to 5 ppm upfield when transferred from water to hexane, while a β-type nitrogen shifts downfield by as much as 15 ppm (*29*).

Protonation and Tautomeric State of Histidines in H24V/H119F Double Mutant Apomyoglobin Monitored by NMR Spectroscopy. Histidine titrations, using ^{1}H−^{15}N HMBC spectra of H24V/H119F double mutant apoMb (Figure 5), indicate that all histidines are fully protonated before the N → I transition occurs at around pH 3.2 (Figure 2). H64 (pK_a = 4.7−4.9) and H48 (pK_a = 5.2−5.4) are the last histidines to titrate (Figure 5). The fact that I is still partially populated in H24V/H119F, as indicated by fluorescence titrations (Figure 2B), argues that titratable groups other than histidines are protonated in the N → I transition.

Titration of Aspartates in Wild-Type and in the H24V/H119F Double Mutant Monitored by ^{1}H−^{13}C NMR Spectroscopy. The seven aspartates in wild-type and H24V/H119F mutant apoMb were selectively labeled with ^{13}C using an auxotrophic *E. coli* strain kindly provided by Professor John Markley (University of Wisconsin at Madison). 2D HBCBCO NMR experiments (*15*, *16*), which correlate the ^{13}C chemical shift of the carboxylate group to the ^{1}H chemical shift of the β-protons, were performed from pH 3.4 to 5.1 for H24V/H119F and from pH 2.0 to 4.2 for WT. Representative spectra are shown in Figures 6 and 7.

For WT, I accounts for more than 90% of all protein molecules at pH 4.2, 4 °C (*17*). Intermediate and unfolded states are in intermediate to fast exchange on the NMR time scale, so that only a population-weighted average chemical shift is detectable. In addition, most of the chemical shift dispersion is lost in I in both proton and carbon dimensions (Figure 6). During pH titration the broad peak for the ^{1}H−^{13}C correlation moves with an apparent pK_a of 3.2 ± 0.2 (Figure 6B) that is identical to the midpoint of the I ⇌ U transition.

Since chemical exchange between N and I is slow on the NMR time scale, separate sets of cross-peaks can be identified for N and I. For H24V/H119F, cross-peaks for N can be detected down to a pH of 3.4 (Figure 7). Only two aspartates, most likely D122 and D20 (or D126) according to proton assignments of Lecomte et al. (*23*), can be followed with confidence for a part of their titration. By use of various values of the fixed end points of the titration curve in fitting the results to the Henderson−Hasselbalch equation, the pK_a was conservatively estimated to lie between 2.9 and 3.6 in N. This pK_a range is only slightly lower than 3.9, the intrinsic pK_a value for the aspartic acid side chain in unfolded proteins (*34*, *35*). Because all peaks shift during the titration, including cross-peaks in spectral regions that are crowded because of overlap with peaks from I, we suggest that none of the seven aspartic acid residues titrates with an unusually low pK_a, e.g. 2, that would be indicative of an energetically significant salt bridge in N.

Modeling the Acid-Induced Unfolding of Apomyoglobin. The acid-induced unfolding of apoMb has been modeled as a three-state reaction, N ⇌ I ⇌ U (*7*, *17*). We have modified the model as described in the Materials and Methods section. The modified model assigns measured pK_a values to the His residues in N, and it allows all proton-binding groups to be protonated, although His 24 is assigned a very low pK_a value. The model is designed to fit the measured CD and fluorescence monitored unfolding curves. Fitted curves are shown in Figure 2 and the pK_a values used are listed in Table 2. Twelve histidines in apoMb are included in the fitting. Individual pK_a values derived from NMR data are used for the pK_a values in N and all histidines are assumed to have the same pK_a of 6.5 for an unperturbed histidine side chain in I. From the NMR data for H24V/H119F (Figure 5), it is clear that histidine protonation does not play a role in the I ⇌ U reactions, and all histidine residues are assigned the same pK_a in U as in I. Limited NMR data suggest pK_a values in the range from 2.9 to 3.7 for aspartates in N (Figure 7). No data are available for the pK_a values in either I or U, and also no data are available for glutamates. The intrinsic pK_a values for aspartate and glutamate side chains are 3.9 and 4.3, respectively, as determined in proteins unfolded by guanidinium chloride (*34*, *35*). This information allowed us to bracket the pK_a values for glutamate and aspartate side chains in N, I, and U. Since no information is available on individual side chains, all glutamates and aspartates are assigned the same pK_a values. More important are differences in pK_a between N, I, and U. Varying the pK_a values

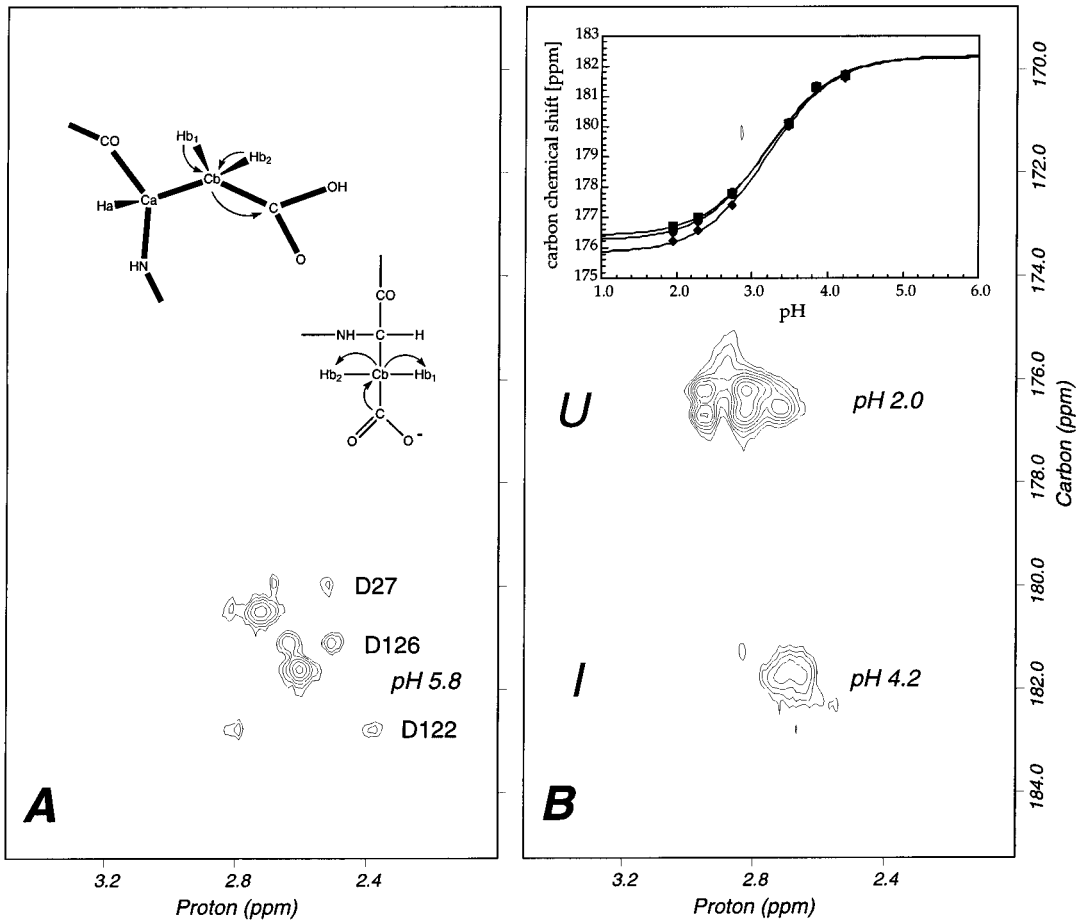

FIGURE 6: $^{1}H-^{13}C-$HBCBCO NMR spectra of selectively ^{13}C-labeled aspartates in wild-type apomyoglobin acquired at 35 °C (2 mM sodium citrate in D_2O) at 600 MHz. (A) Spectra of native wild-type apomyoglobin at pH 5.8. Tentative assignments based on proton assignments by Lecomte and co-workers (*23*) are given for three pairs of cross-peaks. (B) Overlaid are spectra at pH 4.2 and pH 2.0. A broad peak is observed for the $^{13}C-^{1}H\beta$ cross-peaks of all seven aspartates, indicating a mixture of U and I. The ^{13}C chemical shift of the broad feature is plotted as a function of pH in the inset, showing a titration with an apparent pK_a of 3.2. This value is identical to the pH midpoint of the I to U transition monitored by CD and fluorescence spectroscopy.

used in fitting indicates that the ΔpK_a between N and I must lie between 0.1 and 0.3, while a ΔpK_a of 0.2−0.4 adequately describes the I ⇌ U transition. For the fitted curves shown in Figure 2, the pK_a values for all 21 aspartates and glutamates are fixed at 3.3 in N, 3.4 in I, and 3.7 in U. A pK_a value of 3.7 in U is reasonable because Oliveberg et al. (*36*) recently showed that the pK_a values of carboxylate groups in the acid-denatured state of barnase are on average 0.4 unit lower than found for model compounds or for proteins unfolded by guanidinium chloride (*34*, *35*).

Fitting the N ⇌ I transition for wild-type apoMb requires a pK_a value below 4.0 for H24 (3.0 is used in the fitted curves shown in Figure 2). Varying the pK_a of H24 between 1 and 4 does not affect the fit significantly. The N ⇌ I and I ⇌ U reactions of the H24V/H119F double mutant can be adequately modeled by removing H24 and H119 from the model used to fit wild-type. The pK_a values for glutamates and aspartates are kept the same for WT and H24V/H119F. The end points of the unfolding curves monitored by CD and fluorescence are free to float, as are the reference free energy changes. Because I is never fully populated for H24V/H119F, the CD value of its intermediate form is fixed at the value used for the WT. These data are consistent with a simple model in which H24 is not protonated in N and becomes protonated only as the N → I reaction occurs.

DISCUSSION

For many proteins, acid induces partial or complete unfolding. The driving force for the unfolding reaction is the net uptake of protons either by the titration of a few selected side chains or by partial protonation of many different groups (*37*, *38*). In proteins, the pK_a values of side chains may be perturbed considerably from the values of free amino acids or model compounds by electrostatic interactions, by partial burial away from solvent, and by hydrogen bonding. Changes in pK_a values as large as 2 units are not uncommon (*39*). Attempts to calculate pK_a values in proteins of known structure have made considerable progress (*21*, *39*). Here we use heteronuclear NMR methods to obtain pK_a values for histidines and aspartates in sperm whale apoMb and use these values to model its unfolding in acid.

Heteronuclear NMR Spectra Provide a Sensitive Test of the Extent of Protonation and of the Tautomeric State of Histidines. In the $^{1}H-^{15}N$ HMBC spectra, populations of N and I yield separate cross-peaks and they allow the chemical shifts of nine of the 12 histidines in N to be monitored as a function of pH. At pH values above 7, the cross-peaks of most histidines are broadened beyond detection in the ^{15}N dimension but not in the proton dimension; the exceptions are the fully buried histidine H24 and its

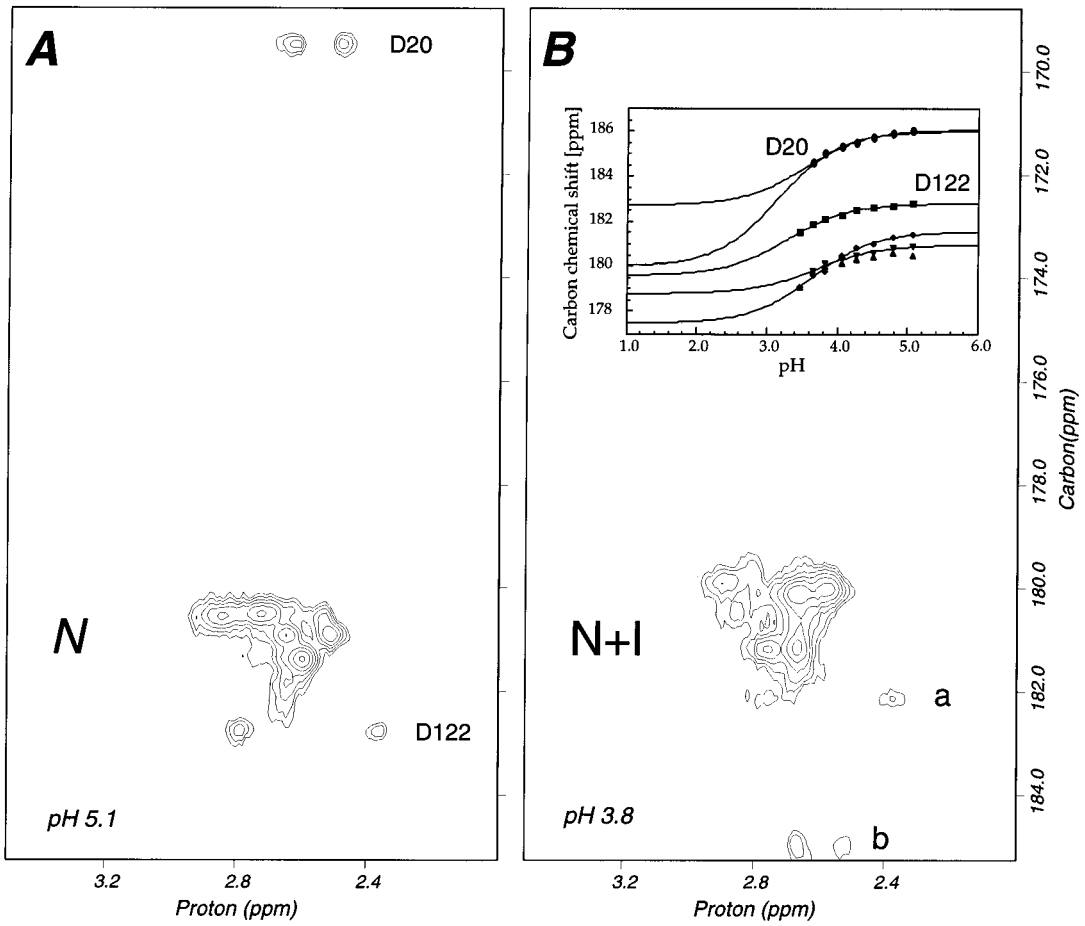

FIGURE 7: $^{1}H-^{13}C$ HBCBCO NMR spectra of selectively ^{13}C-labeled aspartates in H24V/H119F acquired at 35 °C (2 mM sodium citrate in D_2O) at 600 MHz. (A) Spectra of native H24V/H119F at pH 5.1. The pair of cross-peaks at 169.5 ppm are folded from 186 ppm. (B) Spectra at pH 3.8 indicating a mixture of N and I. The two sets of cross-peaks used to estimate the pK_a values are labeled according to proton assignments by Lecomte and co-workers (*23*) tentatively assigned to D122 and D20. D20 β proton chemical shifts are similar to those of D126, leaving some ambiguity. The insert shows the ^{13}C chemical shift of resolved cross-peaks of aspartates in the native state plotted as a function of pH. Fitted lines using the Henderson−Hasselbalch equations are shown, with fixed end points at low pH. The pK_a values are conservatively estimated to lie between 2.9 and 3.7.

hydrogen-bonding partner H119, as well as the fully exposed H48. This broadening of the ^{15}N lines is likely caused by chemical exchange between the two tautomeric forms of solvent-accessible histidines at intermediate rates on the NMR time scale. Because the chemical shifts of the two tautomers differ greatly (250 ppm vs 170 ppm) (Chart 1), this exchange process may cause line broadening in the ^{15}N dimension but not in the proton dimension. At higher pH values the proportion of the second tautomer may increase, as observed for free histidine (*18*, *40*−*42*). Additional broadening caused by protonation/deprotonation (*42*) may explain why the lines of the β-type nitrogen are exchange-broadened over a wide pH range at 25 °C but not at 35 °C. Because of the larger chemical shift difference between exchanging β and α^+ nitrogens, broadening should be larger for the β-type nitrogens than for α nitrogens exchanging with an α^+ nitrogen. For apoMb at pH values above 6.8, both the lines of the α and β-type nitrogens are extremely broadened, which indicates that exchange between tautomeric forms must dominate. Similar behavior has recently been reported for a solvent-exposed histidine in xylanase (*43*). In wild-type apoMb, histidine H24 and H119 can be detected, presumably because their side chains are held rigidly in the δ and ϵ tautomeric states, respectively, by their interactions with each other and with neighboring residues, and also because the exchange with solvent is limited by burial of these side chains. The lines of H48 are also detectable but significantly broader. At high pH the chemical shift of the H48 ϵ2 nitrogen is upfield of most other histidines but similar to that of H119 and H24, whose side chains are buried. Although located at the protein surface, the side chain of H48 appears to be held in place by interactions, possibly with aspartate D44, that are sufficiently strong to prevent tautomerization.

Histidine pK_a Values Are Similar in Apo- and Holomyoglobin Because of Similar Interactions. The pK_a values derived for sperm whale apoMb from $^{1}H-^{15}N$ HMBC NMR data (Figure 4 and Table 1) agree well with those determined from earlier proton NMR studies (*13*, *14*). In addition, the pK_a values of the observable histidines in apoMb are similar to their values in the CO form of holoMb (*21*). This agreement suggests that the molecular environment and interactions in apo- and holoMb are comparable for all histidine residues except those in the heme pocket. In particular, the pK_a of H24 in apoMb appears to be depressed for reasons that are similar to those in holoMb (*21*). The unusually low pK_a of H24 is presumably caused by burial of its side chain and the hydrogen-bonding interaction with H119 (*21*). H119 titrates with a pK_a of 5.9−6.1, a value similar to that determined for holoMb (*21*). After protonation

of H119, the strength of the H24·H119 hydrogen bond increases, as suggested by the downfield shift of the α^+-type H119 ϵ2 nitrogen and the upfield shift of the H24 ϵ2 nitrogen (Figure 4). Strengthening this hydrogen bond decreases the pK_a value of H24 further. In addition, the charged side chain of R118, which is held in position by interactions with aspartates D20 and D27, is positioned directly above the ring of H24. This interaction, and the proximity of other charged groups including K116, reduces the pK_a of H24, as discussed (*21*) for the CO form of holoMb. The core of apoMb that includes the special histidine H24·H119 pair appears to have a structure very similar to that of the holoprotein (*2*, *22*, *23*). For example, Bashford et al. (*21*) correctly predicted the tautomeric arrangement of H24 and H119 observed here, and also in holoMb (*19*), from calculations using the crystal structure of holoMb.

A Subdomain of Apomyoglobin Undergoes Conformational Exchange. The titration behavior of three of the 12 histidine residues could not be followed. These histidines, H97, H93, and H82, are located in helix F on the proximal side of the empty heme binding pocket, and mutating these residues does not affect the pH midpoint of the N ⇌ I reaction of H93G, H97Q, and H82Q apoMb (*7*). This region may undergo conformational exchange in the millisecond time range in N, because the proton NMR lines of these histidine side chains are broadened (*14*). Eliezer and Wright (*22*) recently reported the heteronuclear NMR assignments of sperm whale apoMb at pH 6 but, because of the complete absence of cross-peaks presumably caused by conformational exchange, they could not assign resonances in the EF loop, the F helix, the FG loop, and the beginning of the G helix (Figure 1). In native apoMb, the fluorine NMR lines of fluorinated phenylalanine residues lining the empty heme binding pocket are exchange-broadened beyond detection also (B.H.G., unpublished results). The unusual ^{15}N titration curve of H64 can best be explained if H93 and H97 are nearby, suggesting that the empty heme binding pocket is partially transiently collapsed. The subdomain of apoMb that constitutes the proximal side of the empty heme binding pocket should therefore not be considered unfolded but instead probably makes significant but transient tertiary contacts with the rest of the molecule.

Histidine H119 Titrates While H24 Remains Neutral in the Acid-Induced N → I Reaction. On the basis of the crystal structure of holoMb (*44*) and on neutron diffraction data (*26*), Barrick et al. (*7*) proposed that the special histidine pair H24·H119 "shares" a single delocalized proton at pH values between 6 and the N ⇌ I transition, thereby strongly coupling the titration behavior of H24 and H119 as suggested previously by Bashford et al. (*21*). From their histidine mutant results (nine of the 12 His residues were mutated singly, and the H24V/H119F double mutant was also made), Barrick et al. (*7*) concluded that protonation of the H24·H119 pair plays a key role in causing the N → I reaction. They proposed that, after a first protonation step with a pK_a of 5.3−5.8, H24 and H119 share a proton. The protonation of H24, at the N terminus of the B helix (Figure 1), is expected to strongly destabilize the B helix because of the interaction of a charged histidine with the helix dipole (*45*). Breaking the hydrogen bond between H24 and H119 and protonation of both residues is a plausible explanation for the acid-induced N ⇌ I reaction (*7*).

Scheme 1

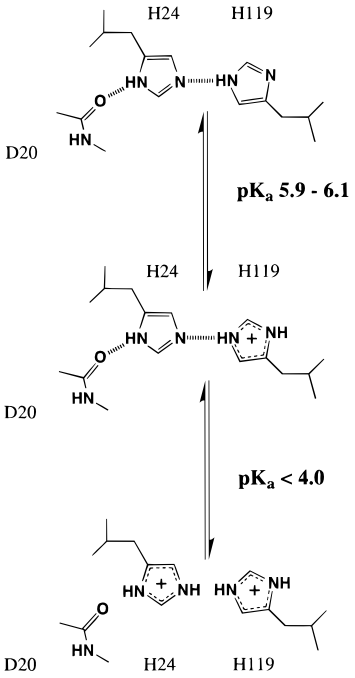

A primary motivation for using ^{1}H−^{15}N NMR to study histidine protonation in apoMb was to investigate the possibility of "proton sharing" in the H24·H119 pair. If sharing occurs, we would expect the cross-peak patterns for H24 and H119 to be at chemical shifts between the two extremes for fully neutral and fully protonated histidine side chains. Instead, the cross-peak patterns observed in the ^{1}H−^{15}N HMBC spectra (Figure 3) unambiguously show that H24 is always in the δ tautomeric form in N and remains neutral even when H119 is protonated (Figures 3 and 4). H119 is in the ϵ tautomer and titrates with a pK_a of 5.9−6.1. Thus, we propose a slightly different protonation scheme for the special H24·H119 pair that includes a first protonation step at H119 with a pK_a of 6.0, followed by a second protonation step of H24, with a pK_a value below 4 (Scheme 1). As will be shown below, the pH dependence of the N ⇌ I reaction can be explained by the protonation of H24 only in I plus some contributions from acidic side chains.

Aspartate Titrations Fail To Detect Strong Side-Chain Interactions. The titration of histidine residues does not play a role in the N to I transition of H24V/H119F because the histidines with the lowest pK_a values, H64 and H48, titrate with pK_a values close to or above 5.0, roughly 1 pH unit above the pH midpoint of the N ⇌ I transition. This fact suggests that other groups, namely, aspartic and glutamic acid residues, are responsible for the N ⇌ I transition in the double mutant. We selectively incorporated ^{13}C-labeled aspartate into wild-type and H24V/H119F and followed the titration of aspartates by heteronuclear NMR methods. Given the limitations of the data (Figures 6 and 7), pK_a values of the aspartate residues in apoMb can conservatively be estimated to lie between 2.9 and 3.7 in N. This suggests that none of the aspartates in H24V/H119F, and presumably none also in wild type, is involved in an interaction that significantly depresses its pK_a value. This conclusion contrasts with calculations by Yang and Honig (*46*), who propose that four of the seven aspartates in apoMb should have pK_a values around or below 2. Likewise, Bashford et

al. (*21*) also predict low pK_a values for some aspartates and glutamates in the holoMb. Currently, mutational studies are underway in our laboratory to test for the presence of salt bridges in apoMb that involve aspartate and glutamate residues.

Acid-Induced Unfolding of Apomyoglobin Is Largely Caused by the Strongly Depressed pK_a of Histidine H24 but Acidic Groups Contribute Also. The driving force for the acid-induced unfolding reaction of a protein is the net uptake of protons, either by the titration of a few selected side chains or by partial protonation of many different groups (*37*, *38*). For the N ⇌ I unfolding reaction, protonation of groups in I will shift the N ⇌ I equilibrium toward I provided that the pK_a values of these groups are lower in N than I. A group whose pK_a in N is greater than its pK_a in I will shift the equilibrium toward N. For that reason, a titrating group that causes a transition at pH 4.4 has to have a pK_a < 4.4 in N but a pK_a > 4.4 in I. Because aspartate and glutamate side chains in unfolded proteins have pK_a values of 3.9 and 4.3, respectively (*34*, *35*), and presumably have lower values in I and N, these groups probably cannot be responsible for causing the N → I reaction in wild-type apoMb whose pH midpoint is 4.4. Of the 12 histidine residues, only histidine H24 has a pK_a value that fits these requirements. Mutating to glutamine the three histidines that are not observable by NMR has little effect on the acid-induced CD unfolding curves (*7*), suggesting that protonation of these His residues is not a key event in the N → I reaction.

To test the effect of H24 mutations, the acid-induced unfolding of apoMb was modeled using the three-state N ⇌ I ⇌ U model (*7*, *17*) using NMR-derived pK_a values of individual, independently titrating groups. The model adequately describes the behavior of WT apoMb and of H24V/H119F. Curves fitted to the CD and fluorescence data (Figure 2) show that the protonation of a single titrating group with a low pK_a in N can qualitatively explain the pH-induced unfolding of WT and H24V/H119F. We suggest (Scheme 1) that protonation of H24 contributes one of the two charges taken up during the N → I reaction (*7*). Uptake of a second proton can be explained by the low pK_a values of other His residues and by the titration of all or a subset of acidic side chains. Fitting the N ⇌ I transition for WT requires a pK_a value below 4.0 for H24, at least 2.5 units below that of an unperturbed histidine side chain. Because the protonation of H24 in I "drives" the N → I reaction, the actual pK_a of H24 in N does not affect the reaction as long as the H24 pK_a is low enough that no measurable protonation occurs in N.

By use of the pK_a values in Table 2, the charge uptake for the titrating groups in the N → I reaction was estimated (Table 3), assuming all pK_a values to be independent of pH. Of the 12 histidines in WT, H24 contributes most to the charge uptake in the transition from fully native protein at pH 5 to maximally populated intermediate at pH 4 (Table 3). All other histidines together (mainly H64 and H48) contribute less than half as much as H24. The protonation of all or a subset of the glutamate and aspartate side chains provides an additional driving force for the N → I reaction. Depending on their actual pK_a values in N and I, the 21 acidic groups in combination may contribute significantly to the charge uptake in going from N to I between pH 5 and 4 (Table 3). The relative energetic contributions of H24 and the acidic groups can only be estimated crudely, however, since the exact pK_a values in N and I are not known. For the H24V/H119F mutant, the N → I reaction is caused almost exclusively by the protonation of glutamates and aspartates (Table 3), and it occurs at lower pH values where the protonation of acidic groups drives unfolding.

Table 3: Proton Uptake Driving Unfolding of Wild-Type and H24V/H119F Apomyoglobin[a]

	$\int \Delta Q^i$ dpH		
residue	wt[b]	wt[c]	H24V/H119F[d]
H12, H81, H82, H93, H97, H116	0	0	0
H36	−0.01	−0.01	−0.001
H113, H119	0.05	0.05	0.001
H48	0.09	0.09	0.02
H64	0.25	0.25	0.15
H24	0.95	0.98	n.a.
D + E (all 21 acidic groups)	0.34	0.74	1.07
sum	1.67	2.11	1.24

[a] Listed are the integrals $\int \Delta Q^i$ dpH, the charge uptake of individual or groups of titrating residues in the transition from N at pH_A to I at pH_B. These integrals reflect the contributions of these residues to the free energy change $\Delta\Delta G_{I-N}(pH) = 2.3RT\int \Delta Q$ dpH (*37*). From Mathematica (Wolfram Research, Inc.), $\int \Delta Q^i$ dpH = $\int \{Q_I^i(pH) - Q_N^i(pH)\}$ dpH; $\int \Delta Q^i$ dpH = $\int [10^{(pK_I^i - pH)}/\{1 + 10^{(pK_I^i - pH)}\} - 10^{(pK_N^i - pH)}/\{1 + 10^{(pK_N^i - pH)}\}]$ dpH; and $\int \Delta Q^i$ dpH = $[\log\{(10^{pH_B} + 10^{pK_I^i})/(10^{pH_A} + 10^{pK_I^i})\} - \log\{(10^{pH_B} + 10^{pK_N^i})/(10^{pH_A} + 10^{pK_N^i})\}]$. For wild-type apomyoglobin, integrals were calculated for $pH_A = 5.0$ and $pH_B = 4.0$. For H24V/H119F apomyoglobin, $pH_A = 3.7$ and $pH_B = 2.7$ were used, because the N ⇌ I transition occurs at lower pH than in wild-type protein. In this pH range, the titration of the histidines does not contribute and the N ⇌ I transition of the H24V/H119F double mutant is exclusively driven by the titration of acidic groups. pK_I^i and pK_N^i are the pK_a values of group *i* in the intermediate (I) and the native state (N), respectively. Calculations assume that the pK_a values are constant and independent of each other, which is clearly an oversimplification. Contributions of individual titrating groups to $\Delta\Delta G$(pH) are additive (*47*). [b] Calculated for the pK_a values listed in Table 2; H24 is assumed to have a pK_a of 3.0 in N, and all 21 acidic groups have a pK_a of 3.3 in N and 3.4 in I. [c] Calculated for a pK_a of 2.0 for H24 in N and pK_a values of 3.3 in N and 3.5 in I for all acidic groups. [d] Calculated for the pK_a values listed in Table 2 except H119 and H24 are removed. All 21 acidic groups have a pK_a of 3.3 in N and 3.4 in I. n.a., not applicable.

In apoMb, the buried histidine H24 has very specific and unique interactions with neighboring side chains, especially H119. These interactions result in a pK_a value for H24 below 4, which greatly stabilizes N against unfolding by acid. A simple model in which H24 becomes protonated in I is sufficient to describe the N ⇌ I transition in WT because acidic groups and other histidines can explain the uptake of a second positive charge in the N ⇌ I transition (*7*). In contrast to the N → I reaction, the I → U reaction is probably caused by the protonation of several or all acidic groups with small pK_a differences between I and U (Kay and Baldwin, unpublished results).

ACKNOWLEDGMENT

We thank Stewart Loh and Michael Kay for helpful advice on protein expression and purification, as well as for comments and discussions. B.H.G. thanks Dr. Joseph Pease and Roche BioSciences, Palo Alto, CA, for the use of their 600 MHz NMR instrument for two test spectra. We thank Professor John Markley (University of Wisconsin, Madison) and co-workers for providing *E. coli* EA-1 cells and the

National NMR Facility at the University of Wisconsin at Madison for the use of their instruments and for staff support.

REFERENCES

1. Griko, Y. V., Privalov, P. L., Venyaminov, S. Y., and Kutyshenko, V. P. (1988) *J. Mol. Biol. 202*, 127−138.
2. Hughson, F. M., Wright, P. E., and Baldwin, R. L. (1990) *Science 249*, 1544−1548.
3. Jennings, P. A., and Wright, P. E. (1993) *Science 262*, 892−896.
4. Kay, M. S., and Baldwin, R. L. (1996) *Nat. Struct. Biol. 3*, 439−445.
5. Jamin, M., and Baldwin, R. L. (1996) *Nat. Struct. Biol. 3*, 613−618.
6. Luo, Y., Kay, M. S., and Baldwin, R. L. (1997) *Nat. Struct. Biol. 4*, 925−930.
7. Barrick, D., Hughson, F. M., and Baldwin, R. L. (1994) *J. Mol. Biol. 237*, 588−601.
8. Pelton, J. G., Torchia, D. A., Meadow, N. D., and Roseman, S. (1994) *Protein Sci. 2*, 543−558.
9. Loh, S., Kay, M. S., and Baldwin (1995) *Proc. Natl. Acad. Sci. U.S.A. 92*, 5446−5450.
10. Maniatis, T., Fritsch, E. F., and Sambrook, J. (1982) *Molecular Cloning: A Laboratory Manual*, Cold Spring Harbor Laboratory Press, Cold Spring Harbor, NY.
11. Bax, A., Ikura, M., Kay, L. E., Torchia, D. A., and Tschudin, R. (1990) *J. Magn. Reson. 86*, 304−318.
12. Shaka, A. J., Keeler, J. Frenkiel, T., and Freeman, R. (1983) *J. Magn. Reson. 52*, 335−338.
13. Cocco, M. J., and Lecomte, J. T. (1994) *Protein Sci. 3*, 267−281.
14. Cocco, M. J., Kao, Y. H., Phillips, A. T., and Lecomte, J. T. (1992) *Biochemistry 31*, 6481−6491.
15. Yamazaki, T., Nicholson, L. K., Torchia, D. A., Wingfield, P., Stahl, S. J., Kaufmann, J. D., Eyermann, C. J., Hodge, C. N., Lam, P. Y. S., Ru, Y., Jadhav, P. K., Chang, Ch.-H., and Weber, P. C. (1994) *J. Am. Chem. Soc. 116*, 10791−10792.
16. Powers, R., Gronenborn, A. M., Clore, G. M., and Bax, A. (1991) *J. Magn. Reson. 94*, 209−213.
17. Barrick, D., and Baldwin, R. L. (1993) *Biochemistry 32*, 3790−3796.
18. Blomberg, F., Maurer, W., and Rüterjans, H. (1977) *J. Am. Chem. Soc. 99*, 8149−8159.
19. Bhattacharya, S., and Lecomte, J. T. (1997) *Biophys. J. 73*, 3241−3256.
20. Bhattacharya, S. Sukits, S. F., MacLaughlin, K. L., and Lecomte, J. T. (1997) *Biophys. J. 73*, 3230−3240.
21. Bashford, D., Case, D. A., Dalvit, C., Tennant, L., and Wright, P. E. (1993) *Biochemistry 32*, 8045−8056.
22. Eliezer, D., and Wright, P. E. (1996) *J. Mol. Biol. 263*, 531−538.
23. Lecomte, J. T. J., Kao, Y.-H., and Cocco, M. J. (1996) *Proteins: Struct., Funct., Genet. 25*, 267−285.
24. Cocco, M. J., and Lecomte, J. T. (1990) *Biochemistry 29*, 11067−11072.
25. Takano, T. (1977) *J. Mol. Biol. 110*, 537−568.
26. Cheng, X., and Schoenborn, B. P. (1991) *J. Mol. Biol. 220*, 381−399.
27. Farr-Jones, S., Wong, W. Y. L., Gutheil, W. G., and Bachovchin, W. W. (1993) *J. Am. Chem. Soc. 115*, 6813−6819.
28. Bachovchin, W. W., and Roberts, J. D. (1978) *J. Am. Chem. Soc. 100*, 8041−8047.
29. Schuster, I. I., and Roberts, J. D. (1979) *J. Org. Chem. 44*, 3864−3867.
30. Roberts, J. D., Yu, C., Flanagan, C., and Birdseye, T. R. (1982) *J. Am. Chem. Soc. 104*, 3945−3949.
31. Bachovchin, W. W. (1986) *Biochemistry 25*, 7751−7759.
32. Bachovchin, W. W., Wong, W. Y. L., Farr-Jones, S., Kettner, C. A., and Shenvi, A. B. (1988) *Biochemistry 27*, 7689−7697.
33. Smith, S. O., Farr-Jones, S., Griffin, R. G., and Bachovchin, W. W. (1989) *Science 244*, 961−964.
34. Nozaki, Y., and Tanford, C. (1967) *J. Am. Chem. Soc. 89*, 742−749.
35. Roxby, R., and Tanford, C. (1971) *Biochemistry 10*, 3348−3352.
36. Oliveberg, M., Arcus, V. L., and Fersht, A. R. (1995) *Biochemistry 34*, 9424−9433.
37. Tanford, C. (1968) *Adv. Protein Chem. 23*, 121−282.
38. Tanford, C. (1970) *Adv. Protein Chem. 24*, 1−95.
39. Antosiewicz, J., McCammon, J. A. and Gilson, M. K. (1996) *Biochemistry 35*, 7819−7833.
40. Alei, M. Jr., Morgan, L. O., Wageman, W. E., and Whaley, T. W. (1980) *J. Am. Chem. Soc. 102*, 2881−2886.
41. Tanokura, M. (1983) *Biochim. Biophys. Acta 742*, 576−585.
42. Sudmeier, J. L., Evelhoch, J. L., and Jonsson, N. B.-H. (1980) *J. Magn. Reson. 40*, 377−390.
43. Plesniak, L. A., Connelly, G. P., Wakarchuk, W. W., and McIntosh, L. P. (1996) *Protein Sci. 5*, 2319−2328.
44. Phillips, S. E. V. (1980) *J. Mol. Biol. 142*, 531−554.
45. Armstrong, K. M., and Baldwin, R. L. (1993) *Proc. Natl. Acad. Sci. U.S.A. 90*, 11337−11340.
46. Yang, A.-S., and Honig, B. (1994) *J. Mol. Biol. 237*, 602−614.
47. Oliveberg, M., Vuilleumier, S., and Fersht, A. R. (1994) *Biochemistry 33*, 8826−8832.
48. Kraulis, P. (1991) *J. Appl. Crystallogr. 24*, 946−950.

BI972516+